International Journal of Medical Microbiology xxx (xxxx) xxx–xxx

Contents lists available at ScienceDirect

International Journal of Medical Microbiology

journal homepage: www.elsevier.com/locate/ijmm

Comparative analyses of biofilm formation among different *Cutibacterium acnes* isolates

Torben Kuehnast[a], Fatih Cakar[a], Theresa Weinhäupl[b], Andreas Pilz[b], Sanja Selak[b], M. Alexander Schmidt[c], Christian Rüter[c], Stefan Schild[a,d,*]

[a] Institute of Molecular Biosciences, University of Graz, Humboldtstraße 50, A-8010, Graz, Austria
[b] ORIGIMM Biotechnology GmbH, Vienna, Austria
[c] Institute of Infectiology, Center for Molecular Biology of Inflammation (ZMBE), University of Münster, Münster, Germany
[d] BioTechMed, Graz, Austria

ARTICLE INFO

Keywords:
Attachment
Cutibacterium acnes
Phylotypes
Skin
Implant
Acne vulgaris

ABSTRACT

The Gram-positive anaerobic bacterium *Cutibacterium acnes* is a commensal of the human skin, but also an opportunistic pathogen that contributes to the pathophysiology of the skin disease acne vulgaris. Moreover, *C. acnes*, in addition to other skin-colonizing bacteria such as *S. epidermidis* and *S. aureus*, is an emerging pathogen of implant-associated infections. Notably, *C. acnes* isolates exhibit marked heterogeneity and can be divided into at least 6 phylotypes by multilocus sequence typing. It is becoming increasingly evident that biofilm formation is a relevant factor for *C. acnes* virulence, but information on biofilm formation by diverse *C. acnes* isolates is limited. In this study we performed a first comparative analysis of 58 diverse skin- or implant-isolates covering all six *C. acnes* phylotypes to investigate biofilm formation dynamics, biofilm morphology and attachment properties to abiotic surfaces. The results presented herein suggest that biofilm formation correlates with the phylotype, rather than the anatomical isolation site. IA1 isolates, particularly SLST sub-types A1 and A2, showed highest biofilm amounts in the microtiter plate assays, followed by isolates of the IC, IA2 and II phylotypes. Microscopic evaluation revealed well-structured three-dimensional biofilms and relatively high adhesive properties to abiotic surfaces for phylotypes IA1, IA2 and IC. Representatives of phylotype III formed biofilms with comparable biomass, but with less defined structures, whereas IB as well as II isolates showed the least complex three-dimensional morphology. Proteinase K- and DNase I-treatment reduced attachment rates of all phylotypes, therefore, indicating that extracellular DNA and proteins are critical for adhesion to abiotic surfaces. Moreover, proteins seem to be pivotal structural biofilm components as mature biofilms of all phylotypes were proteinase K-sensitive, whereas the sensitivity to DNase I-treatment varied depending on the phylotype.

1. Introduction

The Gram-positive, rod-shaped anaerobic, bacterium *Cutibacterium acnes* (formerly known as *Propionibacterium acnes*) is frequently found in sebaceous follicle-rich areas of the human skin. In general, *C. acnes* seems to be well-adapted to its ecological habitat, exemplified by their lysozyme-resistant peptidoglycan, adherence to sebum and efficient utilization of its lipids (Falcocchio et al., 2006; Gribbon et al., 1993; Kamisango et al., 1982). A thick cell wall structure with a high lipid content confers increased resistance to environmental stress including osmotic pressure, ion concentrations, mechanic stress or temperature (Sussman and Tang, 2014).

C. acnes isolates exhibit distinct heterogeneity and are generally classified into different phylogenetic divisions, initially based on serological differentiation and phage typing, later confirmed by sequence analysis of *recA*, *tly* and the CAMP genes. A comprehensive classification system by multilocus sequence typing (MLST) or multiplex touchdown PCR categorized *C. acnes* isolates into the six phylotypes IA1, IA2, IB, IC, II and III (Barnard et al., 2015; Lomholt and Kilian, 2010; McDowell et al., 2012). An alternative single locus sequence typing (SLST) technique allows for quick differentiation of phylotypes into more subtypes, correlating with MLST results (Scholz et al., 2014). Notably, the phylotypes are not equally abundant. Generally, IA1 isolates represent the most abundant phylotype on healthy skin. 39% of the *C. acnes* isolates were identified as IA1, followed by IA2, II and III with ~16 to 18%, and finally IB and IC making up less than 10% of the

* Corresponding author at: Institute of Molecular Biosciences, University of Graz, Humboldtstraße 50, A-8010 Graz, Austria.
E-mail address: stefan.schild@uni-graz.at (S. Schild).

https://doi.org/10.1016/j.ijmm.2018.09.005
Received 30 January 2018; Received in revised form 13 August 2018; Accepted 18 September 2018

skin isolates (McDowell et al., 2012).

Although generally seen as a human skin commensal, *C. acnes* can be considered an opportunistic pathogen associated with invasive infections of the skin, soft tissue, cardiovascular system, deep-organ tissues and implant-associated infections (McGinley et al., 1980). The density of skin colonization with *C. acnes* is highly variable between individuals and is most common in sebaceous follicle-rich areas of the body like forehead, cheeks, neck and shoulders. *C. acnes* is most commonly associated with the skin inflammatory disorder acne vulgaris, which can manifest ranging from mild or transient acne in teenage years to more severe, chronic acne that continues well into adulthood primarily covering the face, shoulders and the back (Achermann et al., 2014). Acne affects not only more than 80% of teenagers, but also a significant percentage of adults who continue to be affected even into their 40s and beyond. *C.* acnes is also a relevant causative agent of implant-associated infections with constantly increasing incidence rates, likely due to improved diagnostic techniques (Aubin et al., 2014). *C.* acnes is frequently isolated from breast implants, implanted cardiovascular devices and, in fact, is currently the most frequently isolated pathogen in prosthetic shoulder joint infections (Achermann et al., 2014). The association of different phylotypes to the diverse diseases caused by *C. acnes* is still under debate by the research community. Notably, the dominance of IA1 among *C. acnes* isolates on human skin is even more pronounced on acne patients ranging from 55% to 74% of all *C. acnes* isolates (Dréno et al., 2018; McDowell et al., 2012; Paugam et al., 2017). Especially, *C. acnes* isolated from follicles or cotton swap of mild or severe acne patients belonged almost exclusively to the IA1 phylotype (Lomholt et al., 2017). This might indicate that acne vulgaris is predominantly associated with type IA1. However, due to limitations of different skin sampling methods which do not sample the same areas of the skin and the fact that the skin of a single individual can be colonized with multiple *C. acnes* strains with different biological and antibiotic resistance properties, it is difficult to link pathogenesis of acne to a single genetic group or isolate (Omer et al., 2017; Sadhasivam et al., 2016). A study analyzing 61 orthopedic implants colonized by *C. acnes* found most frequently phylotype I, followed by type II, while type III could not be detected on any implant (Sampedro et al., 2009). However, a clear association between a specific phylotype and infection of failed orthopedic implants could not be observed (Sampedro et al., 2009). Importantly, a recent report suggests that samples collected from deep tissue infections can be also contaminated by the medical personnel in the progress of surgery due to the great abundance of *C. acnes* on everyone's skin (Mollerup et al., 2016). Thus, false positive detection of *C. acnes* cannot be excluded. The quality of tissue sampling is crucial to avoid false positive detection of *C. acnes* in the future and retrieve better insights in the epidemiology of *C. acnes*.

As pathogenicity of *C. acnes* does not strictly follow Koch's postulates (i.e. cells can be isolated from acne patients and healthy individuals), virulence factors are harder to pinpoint. Based on recent studies biofilm formation emerged as a potential key feature associated with virulence (Coenye et al., 2007; Metiko et al., 2015). In 2004 *in silico* analyses of the first genome sequence available already predicted several gene products to be involved in biofilm formation (Brüggemann et al., 2004). Since then, several studies confirmed the potential of *C. acnes* to readily form biofilms on a variety of surfaces, such as plastic, glass, silicone, titanium and steel (Bayston et al., 2007; Furustrand Tafin et al., 2012; Holmberg et al., 2009). More recently, biofilm aggregates could be visualized in the *stratum corneum* and the hair follicles of acne patients as well as on implant devices (Bayston et al., 2007; Jahns et al., 2012; Tunney et al., 2007). Biofilm formation was proposed to be a key factor in the pathogenesis of acne leading to an increased production of putative virulence factors like extracellular lipases and an elevated resistance of *C. acnes* against antimicrobial agents (Burkhart and Burkhart, 2007a, 2007b; Coenye et al., 2007). Indeed, *C. acnes* biofilm-like aggregates can be more frequently observed in skin biopsies of acne vulgaris patients compared to healthy control groups. Furthermore, *C. acnes* isolates derived from invasive infections have been associated with better biofilm production compared to skin isolates (Holmberg et al., 2009; Jahns et al., 2012). Most importantly and consistent with previous reports on other microorganisms, *C. acnes* biofilms have been shown to be more resistant to antimicrobial killing compared to planktonic bacteria (Coenye et al., 2007; Ramage et al., 2003). Overall these findings point to an important role of biofilm formation in the pathogenesis of *C. acnes*.

Although biofilm formation is nowadays widely accepted as a feature of *C. acnes* pathogenesis, detailed analyses of isolate- and/or phylotype-dependent variations in biofilm formation capacities within the heterogeneous species of *C. acnes* are currently lacking.

In this study we performed the first comprehensive comparative analysis of *C. acnes* isolates covering all 6 phylotypes with regard to the dynamics of biofilm formation, the overall amount of mature biofilms, adhesive properties on abiotic surfaces and biofilm morphology. Finally, the impact of proteinase K- and DNase I-treatment on attachment efficacy and mature biofilms was assessed for representatives all 6 phylotypes to get first insights into the requirements of extracellular or surface-associated DNA and proteins in the initial surface adhesion step and relevant matrix components of three-dimensional biofilms.

2. Materials and methods

2.1. Bacterial strains and growth conditions

A total of 58 *C. acnes* isolates obtained from commercial and academic sources [e.g. Leibniz Institute - German Collection of Microorganisms and Cell Cultures (DSMZ, Braunschweig, Germany), Sheila Patrick at Queen's University Belfast (Northern Ireland, UK), Andrej Trampuz at Pro-Implant Foundation, (Berlin, Germany), István Nagy at Biological Research Centre of the Hungarian Academy of Science (Budapest, Hungary)] were comparatively analyzed in this study (Table S1). The strain collection comprised 29 strains from human skin (healthy individual or acne patients) and 29 from deep tissue or implant-associated infections. All strains were categorized into six phylotypes IA1, IA2, IB, IC, II and III by multiplex touchdown PCR for rapid typing (Barnard et al., 2015; McDowell et al., 2012). IA1 isolates were further sub-classified into SLST types according to Scholz et al. (Scholz et al., 2014). Unless stated otherwise, all strains were incubated at 37 °C anaerobically using AnaeroGen™ 2.5 l (Thermo Scientific) system. At the beginning of each experiment the respective isolates were streaked from −80 °C stocks onto BHI agar plates (Brain Heart Infusion, BD™), incubated for 4 days, resuspended in BHI broth to an appropriate optical density and used as inoculum for the individual experiments.

2.2. Microtiter plate biofilm assay

Biofilm formation dynamics were assayed by crystal violet staining of the attached biomass in 96-well microtiter plates at 72 h, 120 h or 168 h. The protocol is based on previously described assays (Coenye et al., 2007; Holmberg et al., 2009; Seper et al., 2014) with some modifications. A 96-well plate (U-bottom, polystyrene, Sterilin™) was filled with 150 µl per well of the inoculum (OD_{600} = 0.1) and incubated for 72 h, 120 h or 168 h (37 °C, anaerobically). At a given time point, growth of each *C. acnes* isolate was monitored by resuspending the biomass of at least two wells per strain and the measurement of the OD_{600} (SPECTROstar^{Nano}, BGM Labtech). The remaining wells (at least 6 per *C. acnes* isolates) were used for biofilm quantification. The supernatant with the planktonic bacteria was removed and the remaining biofilm was dried for approx. 50 min at 100 °C and surface attached material was fixed by adding 100 µl methanol. After 10 min the methanol was removed, the microtiter plates dried for 30 min at 100 °C and the remaining biofilm was stained with 0.1% crystal violet for 2 min, solubilized in 96% ethanol and the OD_{595} was measured

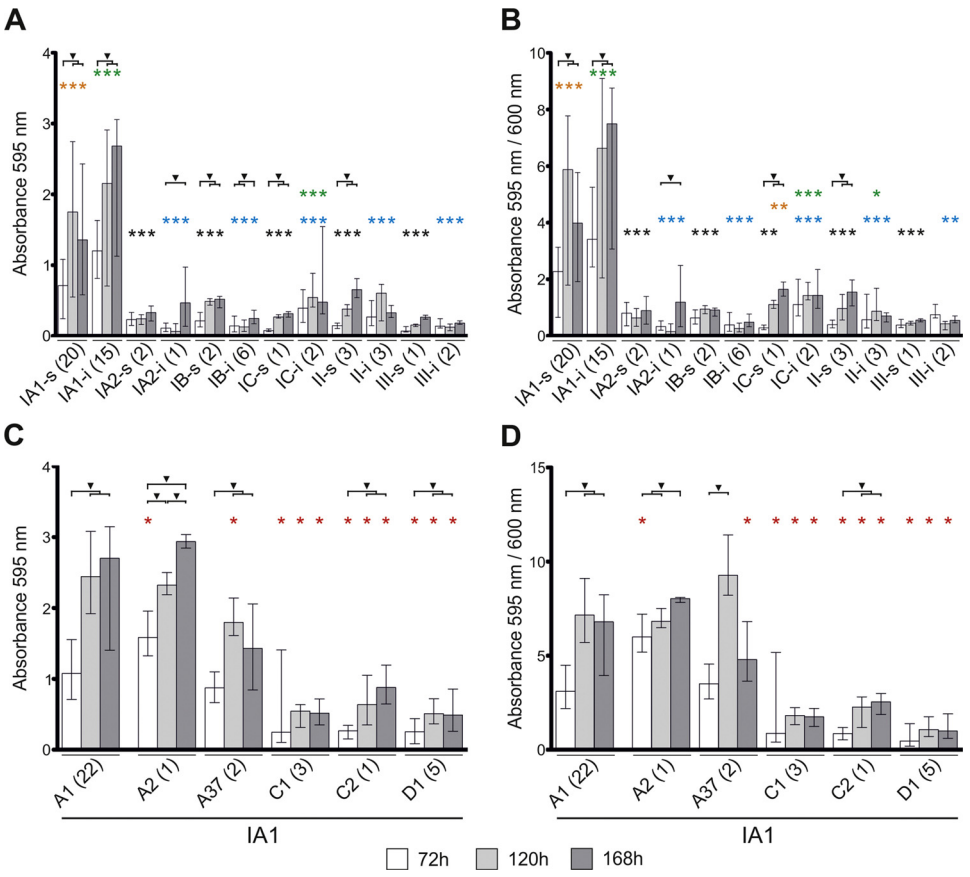

Fig. 1. Biofilm formation of *C. acnes* isolates is phylotype-dependent. (A and B) Shown is the biofilm formation of *C. acnes* isolates categorized into the six phylotypes IA1, IA2, IB, IC, II and III and anatomical isolation sites (-*s* = skin and –i = implant) quantified after 72 h (open bars), 120 h (light gray) and 168 h (dark gray). (C and D) Shown is the biofilm formation of *C. acnes* IA1-*s* and IA1-*i* isolates further discriminated by SLST into the sub-types A1, A2, A37, C1, C2 and D1. The biofilm formation capacity is shown as OD_{595} (A, C) obtained after crystal violet staining or as ratio (B, D) of OD_{595} obtained after crystal violet staining divided by growth determined by OD_{600} measurement to normalize for growth variations (see Material and Methods for details). (A–D) The amount of individual isolates incorporated in each data set is given in parenthesis. 12 independent values from each individual isolate are included in each data set (isolate-specific data sets are provided in Fig. S2). Shown are the medians with interquartile range. Significant differences are indicated as follows ($P < 0.05$, Kruskal-Wallis test followed by post hoc Dunn's multiple comparisons): Significant differences in the biofilm amount of a respective isolates at 72 h, 120 h or 168 h are indicated by black triangles, significant differences of IA1-*s* to other skin-derived isolates at a given time point are indicated by black asterisks, significant differences of IA1-*i* to other implant-derived isolates at a given time point are indicated by blue asterisks, significant differences of IB-s or IB-i to other skin- or implant-derived isolates at a given time point are indicated by orange or green asterisks respectively. Significant differences of A1 to other clusters at a given time point are indicated by red asterisks. (For interpretation of the references to colour in this figure legend, the reader is referred to the web version of this article.)

(SPECTROstar^{Nano}, BMG Labtech) to quantify the amount of biofilm. Wells filled with sterile BHI broth were included in every experiment as a sterile control and served as blank for the OD_{600} and OD_{595} measurements. For each isolate 12 independent values from at least three different microtiter plates were used for the analysis.

2.3. Microscopic visualization of attachment and biofilms

To visualize biofilm morphology 300 µl of the respective inoculum [OD_{600} = 1 (attachment assays) and 0.1 (biofilm assays)] were injected into a three-channel flow-cell chamber (DTU Systems Biology, Technical University of Denmark) with cover slip (24 x 50 mm, Menzel-Glaeser) glued on top as substratum for biofilm growth, and incubated for 1 h aerobically at RT to analyze attachment or 5 days anaerobically at 37 °C to analyze mature biofilms. Afterwards non-attached cells were removed by washing each channel with 3 ml of BHI broth (33 µl/second flow rate), followed by 300 µl BHI broth supplemented with fluorescence dye(s). For detection of DNA of living cells in the attachment and biofilm assays SYTO9 (334 µM) was used. For visualization of live/dead cells the Live/Dead BacLight™ Bacterial Viability kit (Invitrogen) was used according to the manufacturer's protocol. Images of attached cells or biofilms were recorded with an Inverted Microscope Eclipse Ti-E (Nikon™) using either an FITC-3540C or TXRED-4040C filter. Optical sectioning was performed in 0.3 µm steps. For visualization and processing of image data the Leica LAS AF Lite and ImageJ 1.46 software was used. Quantification and morphological analysis of image stacks was performed using the computer program COMSTAT 2 (Heydorn et al., 2000; Vorregaard, 2008).

Attachment was determined by surface coverage evaluation of at least ten images from at least four independent experiments. In case of the three-dimensional analysis of biofilms at least twelve image stacks from four independent experiments with each of the *C. acnes* isolates were used.

2.4. Impact of proteinase K- or DNase I- treatment on C. acnes biofilms and attachment

To test the effect of proteinase K or DNase I on biofilm formation and surface attachment, microtiter plate and flow-cell chamber assays were performed essentially as described above with following modifications: Filter-sterilized stock solutions (10 mg/ml) of proteinase K (Roth, 30 mAnson-U/mg) and DNase I (AppliChem, 5.000U/mg) were prepared freshly in BHI broth prior to each experiment. In case of flow-cell based attachment assays 270 µl of the respective inoculum in BHI broth [OD_{600} = 1.1 (attachment assays)] were treated for 4 h at 37 °C aerobically with 30 µl proteinase K or DNase I solution (final concentration 1 mg/ml each) before the inoculum was injected into a three-channel flow-cell chamber (DTU Systems Biology, Technical University of Denmark) and further processing as described above (see "Microscopic visualization of attachment and biofilms"). An inoculum treated with 30 µl BHI broth served as mock-treated control. In case of flow-cell based biofilm assays, 300 µl of proteinase K or DNase I solution (1 mg/ml in BHI) injected into a three-channel flow-cell chamber containing 5 day old biofilms (BHI, anaerobically at 37 °C) for 4 h at 37 °C before samples were processed as described above (see "Microscopic visualization of attachment and biofilms"). Injection of 300 µl BHI broth served as mock-treated control. In case of microtiter plate assays, biofilms were allowed to grow for 120 h (BHI, anaerobically at 37 °C) before 50 µl of either proteinase K or DNase I solution (in BHI) were added carefully to each well to reach the respective final concentration ranging from to 125 mg/ml to 0.12 ng/ml. Addition of 50 µl BHI broth served as mock-treated control. After incubation at

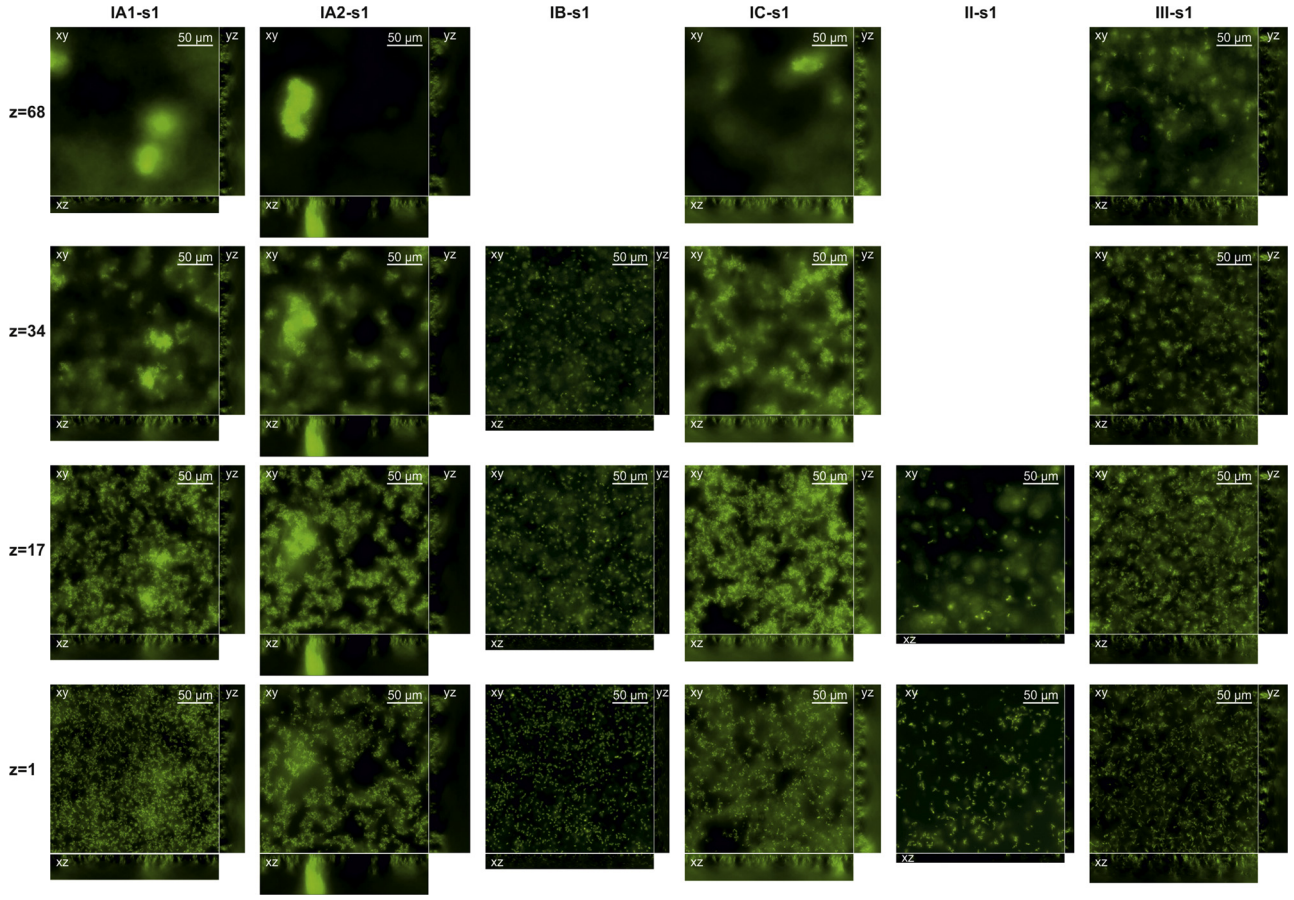

Fig. 2. Comparative morphological analyses of biofilms formed by skin-derived *C. acnes* strains reveal phylotype-dependent architecture. Shown are fluorescent microscopy images of SYTO9 stained *C. acnes* biofilms as horizontal (xy) and vertical (xz and yz) projections (large and side panels, respectively). The respective strain used as representative of the phylotype is indicated on top of each stack. Biofilms were grown for 5 days in flow-cell chambers with BHI broth. Large panels represent selected single optical sections through the acquired three-dimensional data sets at the indicated z position. Optical sectioning was performed in 0.3 µm steps.

37 °C for 4 h aerobically biofilms were washed and processed as described above (see "Microtiter plate biofilm assay").

2.5. Impact of proteinase K- or DNase I- treatment on C. acnes viability

A CFU-based assay was performed to assess effects of proteinase K- or DNase I-treatment on viability of *C. acnes* isolates. 900 µl of *C. acnes* cell culture was adjusted to OD_{600} of 1.1 in BHI broth and mixed with 100 µl of proteinase K or DNase I solution (final concentration 1 mg/ml each) and incubated for 4 h at 37 °C. Addition of BHI broth, instead of either enzyme, served as mock-treated control. Subsequently, appropriate dilutions were plated onto BHI agar plates and incubated for 4 days anaerobically at 37 °C. Plates harboring between 20 and 400 CFUs were used for evaluation. The assay was performed in triplicate.

3. Results and discussion

3.1. Biofilm formation capacity of C. acnes isolates generally correlates with the phylotype classification

A collection of 58 *C. acnes* isolates comprising 29 strains from human skin (healthy individuals or acne patients) and 29 from deep tissue or implant-associated infections were used for comparative analyses of biofilm formation (Table S1). All strains were categorized into the six phylotypes IA1, IA2, IB, IC, II and III by multiplex touchdown PCR for rapid typing (Barnard et al., 2015; McDowell et al., 2012) and consequently labeled as X-YZ (e.g. IA1-s1) in which X stands for the phylotype, Y stands for the point of isolation (i.e. s = skin or i = implant-associated) and Z for the consecutive isolate number (e.g. 1 to 20), respectively. We are aware of the fact that the six phylotypes are not equally represented in this study, but the low abundance of some phylotypes could not be improved by additional isolation rounds. The collection used herein generally reflects the differential abundance of phylotypes (McDowell et al., 2012).

To determine the biofilm formation capacity of diverse *C. acnes* isolates on abiotic surfaces, a microtiter plate biofilm assay was established. A pilot study comprising 31 isolates was performed to identify biofilm dynamics and appropriate growth conditions. Thus, biofilm formation and growth was quantified after anaerobic cultivation for 3–7 days in BHI broth, BHI broth supplemented with 10 mM glucose or thioglycolate (TG) broth, reflecting media compositions frequently used for *C. acnes* cultivation (Furustrand Tafin et al., 2012; Holland et al., 2010; Holmberg et al., 2009). As the diverse *C. acnes* isolates as well as the different media composition exhibited pronounced variations in growth dynamics (Fig. S1), the amount of biofilm detected at a given time was also normalized to the respective growth as assessed by OD_{600} (see Materials and Methods for details.)

Compared to BHI broth, biofilm formation was strongly reduced in TG, likely due to the presence of agar in the TG medium resulting in high viscosity (Fig. S1G and I). Addition of glucose to BHI broth generally resulted in slightly increased biofilm amounts, but also enhanced growth massively. In the majority of cases, the amount of biofilm normalized to growth was therefore equal or even lower compared to regular BHI broth (Fig. S1D, E and F). Thus, regular BHI broth was used

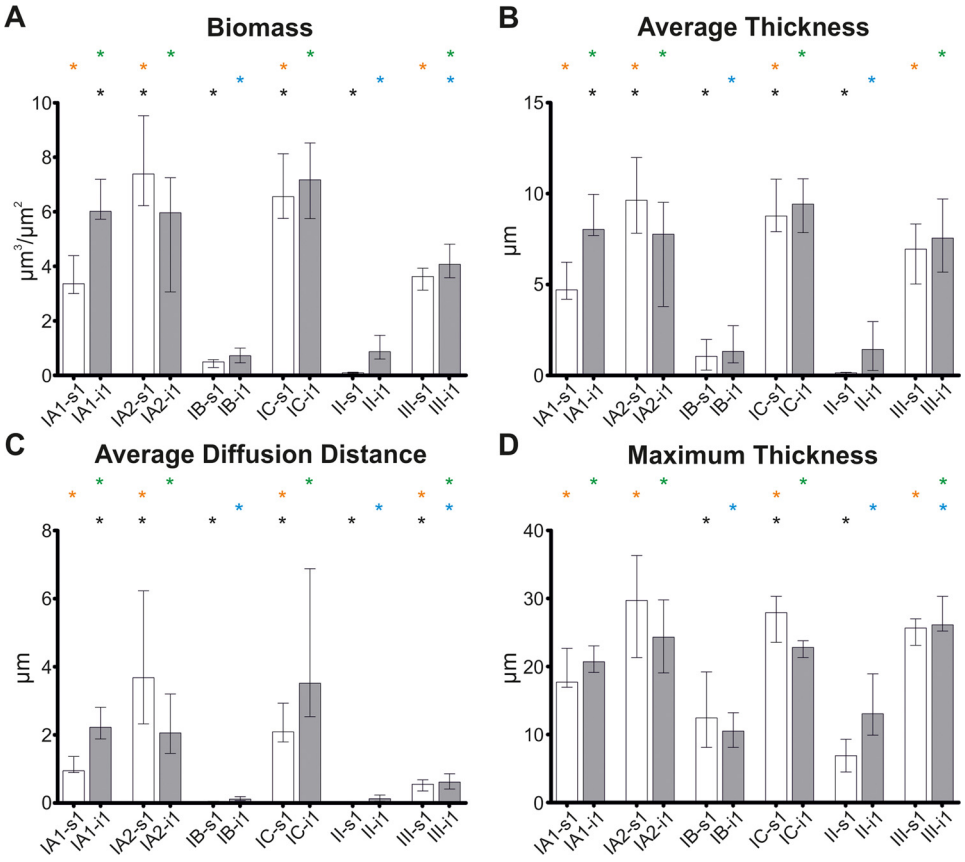

Fig. 3. Analyses of the *C. acnes* biofilm morphology by COMSTAT reveal phylotype-dependent characteristics. Image stacks of respective isolates were analyzed for the biomass (A), the average thickness (B), the average diffusion distance (C) and the maximum thickness (D) using the COMSTAT 2 software (Heydorn et al., 2000; Vorregaard, 2008). Shown are the medians of at least ten image stacks from at least four independent experiments for each strain. The error bars indicate the interquartile range. Significant differences are indicated by asterisks for the following comparisons ($P < 0.05$, Kruskal-Wallis test followed by post hoc Dunn's multiple comparisons): Significant differences of IA1-s1 to IA1-i1 or other skin-derived isolates (open bars) are indicated by black asterisks, significant differences of IA1-i1 to other implant-derived isolates (grey bars) are indicated by blue asterisks, significant differences of IB-s1 to IB-i1 or other skin-derived isolates are indicated by orange asterisks, significant differences of IB-i1 to other implant-derived isolates are indicated by green asterisks. (For interpretation of the references to colour in this figure legend, the reader is referred to the web version of this article.)

in all assays throughout this study.

Biofilm formation was quantified at 72 h, 120 h and 168 h to monitor the biofilm formation dynamics of the different *C. acnes* isolates (Fig. S2). In case of *C. acnes* isolates with low biofilm formation, maximum levels were already reached at 72 h. In contrast, isolates with robust biofilm formation generally showed an increase in biofilm production from 72 h to 120 h, but then leveled off and showed no further increase from 120 h to 168 h. As for most isolates biofilm formation did not significantly increase between 120 h to 168 h. The investigated period likely covered biofilm formation up to mature biofilms.

To analyze whether the capacity for biofilm formation depends on the phylotype or the anatomical site of isolation (skin or implant), all 58 strains were sorted into the respective groups (Fig. 1). Although isolates of a particular phylotype exhibited a distinct heterogeneity in biofilm formation, there were obvious differences between the phylotypes. IA1 isolates from skin and implants formed significantly more biofilm, 2–8 fold more than other phylotypes in almost all cases (Fig. 1A and B, black and blue asterisks). Similar patterns of biofilm formation with and without normalization to growth were observed suggesting that growth differences of the different isolates have only minor impact on the overall biofilm production (Fig. 1A and B). Based on median biofilm levels, IA1 strains were followed by IC, IA2 and II isolates, whereas isolates of the IB and III phylotype showed the lowest biofilm formation in these assays. However, it should be noted that the differences in biofilm formation among non-IA1 phylotypes were rather small. In the case of IB isolates, which represented bad biofilm producers in this assay, significantly increased biofilm formation was only detected for IA1 at all time points, for IC isolates at some time points and for implant associated II at one time point (Fig. 1A and B, green and orange asterisks).

In general, the site of isolation had no significant impact on the biofilm formation capacity. Notably, implant-derived IA1 strains (IA1-i) showed slightly, but not significantly increased biofilm amounts compared to the skin-derived IA-1 strains (IA1-s), especially at 168 h. In summary, biofilm formation predominantly depended on the phylotype and not on the anatomical site of isolation.

As the variation in biofilm formation of IA1 isolates was quite high, all available IA1 strains were further classified by SLST into sub-types (Fig. 1C and D). This reduced the variation, with highest biofilm amounts produced by sub-type A1 (22 isolates) and A2 (1 isolate), both corresponding to MLST clade CC18 of the Aarhus scheme or CC-1 of the Belfast scheme, respectively (Lomholt and Kilian, 2010; McDowell et al., 2012). Sub-types C1, C2 (corresponding to CC-3 in the Aarhus and Belfast scheme) and D1 (corresponding to CC28 of the Aarhus scheme or CC-4 of the Belfast scheme, respectively) showed significantly lower biofilm formation compared to A1. Thus, the higher biofilm formation capacity of IA1 mainly relies on sub-types A1, A2 and the herein new identified sub-type A37. It was previously reported that the clades CC3, CC18 and CC28 as well as sequence type ST18 within the clade CC18 are strongly associated with moderate to severe acne (Kilian et al., 2012; Lomholt and Kilian, 2010). Our results indicate that isolates of these clades show significantly more biofilm production in the microtiter plate biofilm assay.

3.2. *C. acnes* phylotypes show characteristic biofilm morphology

Besides dynamic biofilm quantification, the morphology of biofilms was also investigated using fluorescent microscopy. Whereas the microtiter plate assay is applicable for high-throughput analyses, microscopic analyses are more labor-intensive and time consuming. Therefore, we focused on reference strains as representatives of the six phylotypes and two anatomical isolation sites. Each reference strain was selected based on the individual dynamic biofilm formation, which matched the corresponding median values of the respective phylotype best (Fig. S2). For microscopic analysis biofilms were allowed to form for 120 h as the majority of *C. acnes* isolates' biofilm levels reached a

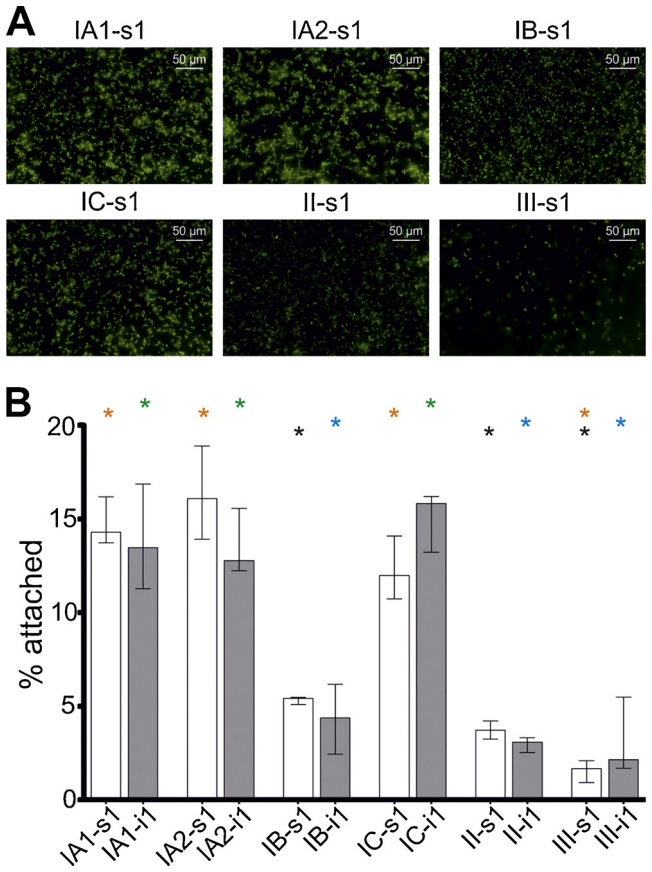

Fig. 4. Adhesive properties of *C. acnes* isolates to abiotic surfaces. Shown are representative microscopic images of skin-derived reference strains (A) and median surface coverage (B) determined by the COMSTAT 2 software (Heydorn et al., 2000; Vorregaard, 2008) for all twelve reference strains. *C. acnes* cells were allowed to attach for 1 h, before non-attached cells were removed and the attached cells were stained with SYTO 9. Micrographs represent a single optical section to visualize the surface coverage on the cover slip. For each isolate at least ten images from four independent experiments were analyzed. The error bars indicate the interquartile range. Significant differences are indicated by asterisks for the following comparisons ($P < 0.05$, Kruskal-Wallis test followed by post hoc Dunn's multiple comparisons): Significant differences of IA1-s1 to IA1-i1 or other skin-derived isolates (open bars) are indicated by black asterisks, significant differences of IA1-i1 to other implant-derived isolates (grey bars) are indicated by blue asterisks, significant differences of IB-s1 to IB-i1 or other skin-derived isolates are indicated by orange asterisks, significant differences of IB-i1 to other implant-derived isolates are indicated by green asterisks. (For interpretation of the references to colour in this figure legend, the reader is referred to the web version of this article.)

plateau or peaked at this time point (Fig. S2). A life/dead staining using propidium iodide and SYTO9 fluorescent dyes indicated a vital biofilm for all isolates tested with only a few dead cells found at the bottom of the biofilm (Fig. S3).

Representative images of biofilms formed by skin- and implant-derived reference strains of all six phylotypes are provided in Fig. 2 and S4, respectively. Image stacks of independently grown biofilms of each reference strain were also evaluated for defined biofilm parameters by COMSTAT 2 software (Fig. 3) (Heydorn et al., 2000; Vorregaard, 2008). Skin- and implant-derived reference strains of the phylotypes IA1, IA2 and IC formed well-structured three-dimensional biofilms with distinct pillars and fluid-filled caverns and channels (Figs. 2 and S4). Defined multicellular aggregates are highlighted by relative high average diffusion distances (Fig. 3C), providing a measure for the shortest average distance from a cell in the biofilm to a fluid-filled channel. Reference strains of phylotype III formed biofilms with similar thickness and biomass, but less defined cell aggregates and pillars indicated by a reduced average diffusion distance compared to IA1, IA2 and IC (Fig. 3). Biofilms of IB and II phylotype strains showed the least structured three-dimensional morphology with almost no cell aggregates, relatively low biomass and thin biofilms (Figs. 2, 3 and S4).

The microscopic analyses allowed for a more refined characterization of the capacity for biofilm formation. While the microtiter plate assay incorporates several stringent washing steps to remove unattached cells and remaining traces of crystal violet, the processing of mature biofilms for the microscopic evaluation is more gentle. Thus, fragile biofilms with low adhesive properties are better preserved in the microscopy chamber, but more likely to be destroyed in the microtiter plate assay. This could explain the relatively high biofilm levels of IA2, IC and III isolates only observed only by the microscopic analyses and emphasizes the necessity to investigate biofilm formation via different approaches.

Consistent with the results of the microtiter plate assay, the biofilm morphology correlated more with the phylotype than with the anatomical isolation point. In further concordance with the microtiter assays, implant-derived IA1-i1 isolate exhibited slightly increased biomass, average thickness and diffusion distance values compared to the skin-derived IA1-s1. A similar result can be observed for phylotype II. It could be hypothesized that implant-derived IA1 and II isolates have a slightly increased biofilm formation capacity compared to skin isolates of the same phylotype. Interestingly, Holmberg et al. recently reported that invasive isolates of *C. acnes* produce more biofilm compared to superficial skin isolates (Holmberg et al., 2009). Although this study used a less comprehensive phylotyping scheme, more than 50% of their isolates were categorized in the IA group followed by group II with approximately 30%. Thus, the study likely investigated predominantly IA1 and II isolates. Furthermore, the results of both studies might indicate that invasive, implant-derived IA1 and II isolates have an increased biofilm formation capacity compared to skin-derived IA1 isolates or that their biofilm formation capacity may be differentially modulated in specific environments, showing more biofilm formation under the conditions applied in these studies (i.e. BHI broth). The pathophysiological relevance of these findings requires further investigation.

3.3. Abiotic attachment of *C. acnes* isolates correlates with the phylotype classification

As attachment to abiotic surfaces is considered to be the first step in biofilm formation, the ability to cover an abiotic surface within 1 h was assessed for the skin- and implant-derived reference strains (Figs. 4 and S5). IA1, IA2 and IC isolates which formed a well-structured three-dimensional biofilm (Figs. 2 and S4) showed a similar, relatively high median surface coverage of ~15% (Fig. 4). In contrast, isolates of groups IB, II and III exhibited low attachment properties with a median surface coverage of 5% or less (Fig. 4). No obvious differences between skin- or implant-derived isolates within the same phylotype could be observed.

3.4. *C. acnes* biofilms and attachment to abiotic surfaces depend on extracellular DNA (eDNA) and proteins

The biofilm matrix of *C. acnes* strain KPA171202 (type IB) is composed of carbohydrates, proteins and eDNA (Jahns et al., 2016). These macromolecules may not only be important as structural components for mature biofilms, but can also play critical roles in the initial surface attachment. The flow-cell chamber assays established in this study were used to investigate the impact of proteinase K or DNase I-treatment on biofilm structure and surface attachment of reference strains for the six *C. acnes* phylotypes. The concentration of both enzymes was adjusted to 1 mg / ml to ensure effective degradation of accessible protein or DNA without adverse effects on cell viability. The latter was verified by

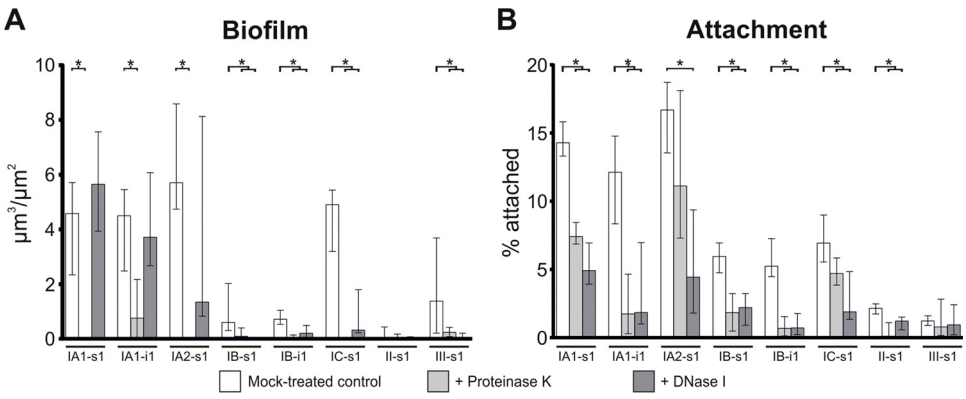

Fig. 5. Impact of Proteinase K and DNase I-treatment on biofilms and abiotic surface adhesion of *C. acnes*. (A) Biofilms were grown for 5 days in flow-cell chambers with BHI broth and subsequently incubated for 4 h with 1 mg/ml proteinase K (light gray), 1 mg/ml DNase I (dark gray,) or mock-treated with BHI broth (open bars), before non-attached cells were removed and the attached cells were stained with SYTO 9. Fluorescent image stacks were acquired to analyze the biomass using the COMSTAT 2 software (Heydorn et al., 2000; Vorregaard, 2008). Shown are the medians of at least ten image stacks from at least four independent experiments for each strain. The error bars indicate the interquartile range. (B) *C. acnes* cells were incubated for 4 h with 1 mg/ml proteinase K (light gray), 1 mg/ml DNase I (dark gray,) or mock-treated with BHI broth (open bars), before they were allowed to attach for 1 h in flow-cell chambers. Subsequently, non-attached cells were removed and the attached cells were stained with SYTO 9 to acquire representative microscopic images for analysis of the median surface coverage using the COMSTAT 2 software (Heydorn et al., 2000; Vorregaard, 2008). Shown are the medians of at least ten images from at least four independent experiments for each strain. The error bars indicate the interquartile range.
(A and B) Significant differences in biomass or attachment between mock-treated control and proteinase K- or DNase I-treated samples are indicated by asterisks ($P < 0.05$, Kruskal-Wallis test followed by post hoc Dunn's multiple comparisons).

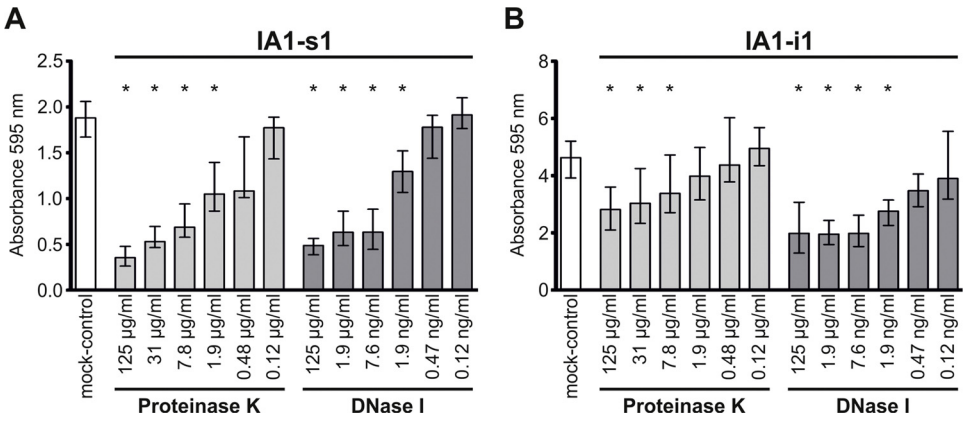

Fig. 6. Impact of Proteinase K and DNase I-treatment on biofilms in the microtiter plate assay. Biofilms were allowed to form for 120 h in the microtiter plate assay with BHI broth for reference isolates IA1-s1 (A) and IA1-i1 (B) and subsequently incubated for 4 h with serial dilutions of proteinase K (light gray), DNase I (dark gray,) or mock-treated with BHI broth (open bars). Shown are the medians with interquartile range. At least 32 independent values were included for each data set. Significant reduction compared to the mock-treated control is indicated by an asterisk ($P < 0.05$, Kruskal-Wallis test followed by post hoc Dunn's multiple comparisons).

performing a CFU viability assay, where cells were exposed to DNase I and proteinase K for 4 h at 37 °C, simulating the same condition used in the biofilm or attachment assays. No significant decrease in the CFU count of DNase I or proteinase K-treated cells was observed in comparison to the mock-treated control for any reference *C. acnes* strain (Fig. S6). Treatment of mature biofilms with proteinase K resulted in most cases in significant reduction of the biofilm biomass (Fig. 5A). In the majority of cases, the biofilm was completely destroyed. Only for II-s1, which produced almost no detectable biofilm, no significant reduction of the biofilm biomass upon proteinase K-treatment could be observed. In contrast, treatment with DNase I was only effective against mature biofilms of IB, IC and III, whereas IA1 biofilms were fairly resistant to DNase I activity. Thus, the results indicate a phylotype-dependent difference in DNase I-sensitivity of mature *C. acnes* biofilms. With regard to the surface adhesion, proteinase K- and DNase I-treatment significantly impaired attachment properties of almost all *C. acnes* strains independent of the phylotype (Fig. 5B). Hence, proteins and eDNA seem to contribute to the initial surface attachment of *C. acnes*.

The impact of DNase I- and proteinase K-treatment was also assessed in the microtiter plate biofilm assays (Fig. 6). Using this high-throughput assay, we were able to test effects of several different enzyme concentrations. However, the assay was limited to IA1 isolates, as only these showed decent biofilm formation in microtiter plates. In contrast to the flow-cell based assay, IA1 biofilms in the microtiter plates were susceptible to both, DNase I- and proteinase K-treatment. In comparison to the mock-treated control significant reductions in the biofilm amount were observed with proteinase K concentrations down to 1.9 µg/ml and DNase I concentrations down to 1.9 ng/ml. As already discussed above, the microtiter plate assay employed more stringent washing steps, while the processing of biofilms for the microscopic evaluation was more gentle. We, therefore, speculate that DNase I-treatment in combination with the more intense washing steps during the microtiter plate assay had a stronger negative effect on the adhesive properties of the biofilm, compared to the same treatment performed under the assay conditions inside the microscopy chamber. In this context, the microtiter plate assay seems to be a stronger indicator of the factors, which are relevant for the biofilm attachment to the abiotic surface.

4. Concluding remarks

It is becoming increasingly evident that biofilm formation is an important feature for *C. acnes* pathogenesis of skin diseases and implant-associated infections. *C. acnes* isolates are characterized by a high genetic heterogeneity, which allows the classification into different phylotypes and sub-types. This work provides a first comparative analysis of in vitro biofilm formation capacities using a comprehensive collection of *C. acnes* isolates comprising representatives categorized by phylotypes (IA1, IA2, IB, IC, II and III), IA1 SLST sub-types and anatomical isolation site (skin and implant). In this study we focused on reproducible microtiter plate and flow-cell chamber assays, which have been frequently used to investigate biofilm formation of other bacteria. Naturally, such in vitro biofilm assays have limitations in regard to the in vivo situation. Thus, future studies will be required to test whether all the observations presented herein can be transferred to in vivo biofilm formation. In the microtiter plate assay, which employed more

stringent washing steps, skin- and implant-derived IA1 isolates showed 2–8-fold higher biofilm formation capacity compared to other phylotypes. In particular, SLST sub-types A1 and A2 exhibit high biofilm formation capacity, which is an interesting finding considering that these sub-types were shown to have a stronger association with mild to severe acne. Microscopic analyses of the biofilm morphologies allowed visualization and evaluation of the three-dimensional biofilm structures. This resulted in a more refined assessment of biofilm formation by diverse *C. acnes* isolates, with well-structured mature biofilms formed by phylotypes IA1, IB, and IC. Concordantly, these isolates also showed the highest attachment rates to abiotic surfaces. In general, no consistent differences in biofilm formation between skin- and implant-derived isolates of the same phylotype could be observed. A notable exception is the IA1 phylotype, with slightly higher biofilm values of implant-derived isolates compared to skin-derived isolates in both assays. Proteinase K- and DNase I-sensitivity assays revealed that both, eDNA and proteins, are important for initial attachment to abiotic surfaces and that proteins are important structural components of the mature biofilms formed by all phylotypes. In contrast, a phylotype-dependent difference in DNase I-sensitivity of mature *C. acnes* biofilms could be observed. Taken together, the results presented herein indicate that biofilm formation by *C. acnes* is primarily dictated by the phylotype and to a much lower extent by the anatomical site of isolation. A potential epidemiological and pathophysiological impact of these findings needs to be addressed in future studies.

Conflict of interest

Sanja Selak is a managing director, CSO and shareholder of ORIGIMM Biotechnology, a privately owned company developing therapeutic products against *C. acnes*-associated infections. Theresa Weinhäupl and Andreas Pilz contributed to this study as employees of ORIGIMM Biotechnology.

Acknowledgements

The authors wish to thank Sheila Patrick at Queen's University Belfast (Northern Ireland, UK), Andrej Trampuz at Pro-Implant Foundation (Berlin, Germany) and István Nagy at Biological Research Centre of the Hungarian Academy of Science (Budapest, Hungary) for generously providing additional *C. acnes* isolates for our studies.

The work was supported by the Austrian Research Promotion Agency (FFG) Basis project 853729 as well as Austrian Science Fund (FWF) grants P27654 to S.S and W901 (DK Enzymology) to F.C. and S.S. Further support came from the Deutsche Forschungsgemeinschaft (DFG, RU1884/2-1 to C.R., SFB1009 TP B03 to C.R. and M.A.S.), the Cells-in-Motion Cluster of Excellence (EXC 1003-CiM), and by a Grant from the Interdisciplinary Centre for Clinical Research (IZKF, Rüt2/002/16 to C.R.) of the Medical Faculty of the University of Muenster.

Appendix A. Supplementary data

Supplementary material related to this article can be found, in the online version, at doi:https://doi.org/10.1016/j.ijmm.2018.09.005.

References

Achermann, Y., Goldstein, E.J.C., Coenye, T., Shirtliff, M.E., 2014. *Propionibacterium acnes*: from commensal to opportunistic biofilm-associated implant pathogen. Clin. Microbiol. Rev. 27 (3), 419–440.

Aubin, G.G., Portillo, M.E., Trampuz, A., Corvec, S., 2014. *Propionibacterium acnes*, an emerging pathogen: from acne to implant-infections, from phylotype to resistance. Med. Mal. Infect. 44 (6), 241–250.

Barnard, E., Nagy, I., Hunyadkurti, J., Patrick, S., McDowell, A., 2015. Multiplex touchdown PCR for rapid typing of the opportunistic pathogen Propionibacterium acnes. J. Clin. Microbiol. 53 (4), 1149–1155.

Bayston, R., Ashraf, W., Barker-Davies, R., Tucker, E., Clement, R., Clayton, J., Freeman, B.J.C., Nuradeen, B., 2007. Biofilm formation by *Propionibacterium acnes* on biomaterials in vitro and in vivo: impact on diagnosis and treatment. J. Biomed. Mater. Res. A 81 (3), 705–709.

Brüggemann, H., Henne, A., Hoster, F., Liesegang, H., Wiezer, A., Strittmatter, A., Hujer, S., Durre, P., Gottschalk, G., 2004. The complete genome sequence of *Propionibacterium acnes*, a commensal of human skin. Science (New York, N.Y.) 305 (5684), 671–673.

Burkhart, C.G., Burkhart, C.N., 2007a. Expanding the microcomedone theory and acne therapeutics: *Propionibacterium acnes*biofilm produces biological glue that holds corneocytes together to form plug. J. Am. Acad. Dermatol. 57 (4), 722–724.

Burkhart, C.G., Burkhart, C.N., 2007b. Treatment of acne vulgaris without antibiotics: tertiary amine-benzoyl peroxide combination vs. benzoyl peroxide alone (Proactiv Solution). Int. J. Dermatol. 46 (1), 89–93.

Coenye, T., Peeters, E., Nelis, H.J., 2007. Biofilm formation by *Propionibacterium acnes* is associated with increased resistance to antimicrobial agents and increased production of putative virulence factors. Res. Microbiol. 158 (4), 386–392.

Dréno, B., Pécastaings, S., Corvec, S., Veraldi, S., Khammari, A., Roques, C., 2018. *Cutibacterium acnes* (*Propionibacterium acnes*) and acne vulgaris: a brief look at the latest updates. J. Eur. Acad. Dermatol. Venereol.: JEADV 32 (Suppl. 2), 5–14.

Falcocchio, S., Ruiz, C., Pastor, F.J., Saso, L., Diaz, P., 2006. *Propionibacterium acnes* GehA lipase, an enzyme involved in acne development, can be successfully inhibited by defined natural substances. J. Mol. Catal. B Enzym. 40 (3–4), 132–137.

Gribbon, E.M., Cunliffe, W.J., Holland, K.T., 1993. Interaction of *Propionibacterium acnes* with skin lipids in vitro. J. Gen. Microbiol. 139 (8), 1745–1751.

Heydorn, A., Nielsen, A.T., Hentzer, M., Sternberg, C., Givskov, M., Ersbøll, B.K., Molin, S., 2000. Quantification of biofilm structures by the novel computer program COMSTAT. Microbiology (Reading, England) 146 (Pt 10), 2395–2407.

Holland, C., Mak, T.N., Zimny-Arndt, U., Schmid, M., Meyer, T.F., Jungblut, P.R., Bruggemann, H., 2010. Proteomic identification of secreted proteins of Propionibacterium acnes. BMC Microbiol. 10, 230.

Holmberg, A., Lood, R., Morgelin, M., Soderquist, B., Holst, E., Collin, M., Christensson, B., Rasmussen, M., 2009. Biofilm formation by *Propionibacterium acnes* is a characteristic of invasive isolates. Clin. Microbiol. Infect. 15 (8), 787–795.

Jahns, A.C., Lundskog, B., Ganceviciene, R., Palmer, R.H., Golovleva, I., Zouboulis, C.C., McDowell, A., Patrick, S., Alexeyev, O.A., 2012. An increased incidence of *Propionibacterium acnes* biofilms in acne vulgaris: a case-control study. Br. J. Dermatol. 167 (1), 50–58.

Jahns, A.C., Eilers, H., Alexeyev, O.A., 2016. Transcriptomic analysis of *Propionibacterium acnes* biofilms in vitro. Anaerobe 42, 111–118.

Kamisango, K., Saiki, I., Tanio, Y., Okumura, H., Araki, Y., Sekikawa, I., Azuma, I., Yamamura, Y., 1982. Structures and biological activities of peptidoglycans of *Listeria monocytogenes* and *Propionibacterium acnes*. J. Biochem. 92 (1), 23–33.

Kilian, M., Scholz, C.F.P., Lomholt, H.B., 2012. Multilocus sequence typing and phylogenetic analysis of Propionibacterium acnes. J. Clin. Microbiol. 50 (4), 1158–1165.

Lomholt, H.B., Kilian, M., 2010. Population genetic analysis of *Propionibacterium acnes* identifies a subpopulation and epidemic clones associated with acne. PLoS One 5 (8), e12277.

Lomholt, H.B., Scholz, C.F.P., Brüggemann, H., Tettelin, H., Kilian, M., 2017. A comparative study of *Cutibacterium* (*Propionibacterium*) *acnes* clones from acne patients and healthy controls. Anaerobe 47, 57–63.

McDowell, A., Barnard, E., Nagy, I., Gao, A., Tomida, S., Li, H., Eady, A., Cove, J., Nord, C.E., Patrick, S., 2012. An expanded multilocus sequence typing scheme for *propionibacterium acnes*: investigation of' pathogenic',' commensal' and antibiotic resistant strains. PLoS One 7 (7), e41480.

McGinley, K.J., Webster, G.F., Ruggieri, M.R., Leyden, J.J., 1980. Regional variations in density of cutaneous propionibacteria: correlation of *Propionibacterium acnes* populations with sebaceous secretion. J. Clin. Microbiol. 12 (5), 672–675.

Metiko, B., Brooks, K., Burkhart, C.G., Burkhart, C.N., Morrell, D., 2015. Is the current model for acne pathogenesis backwards? J. Am. Acad. Dermatol. 72 (6), e167.

Mollerup, S., Friis-Nielsen, J., Vinner, L., Hansen, T.A., Richter, S.R., Fridholm, H., Herrera, J.A.R., Lund, O., Brunak, S., Izarzugaza, J.M.G., Mourier, T., Nielsen, L.P., Hansen, A.J., 2016. *Propionibacterium acnes*: disease-causing agent or common contaminant? Detection in diverse patient samples by next-generation sequencing. J. Clin. Microbiol. 54 (4), 980–987.

Omer, H., McDowell, A., Alexeyev, O.A., 2017. Understanding the role of *Propionibacterium acnes* in acne vulgaris: the critical importance of skin sampling methodologies. Clin. Dermatol. 35 (2), 118–129.

Paugam, C., Corvec, S., Saint-Jean, M., Le Moigne, M., Khammari, A., Boisrobert, A., Nguyen, J.M., Gaultier, A., Dréno, B., 2017. *Propionibacterium acnes*phylotypes and acne severity: An observational prospective study. J. Eur. Acad. Dermatol. Venereol.: JEADV 31 (9), e398–e399.

Ramage, G., Tunney, M.M., Patrick, S., Gorman, S.P., Nixon, J.R., 2003. Formation of *Propionibacterium acnes* biofilms on orthopaedic biomaterials and their susceptibility to antimicrobials. Biomaterials 24 (19), 3221–3227.

Sadhasivam, S., Sinha, M., Saini, S., Kaur, S.P., Gupta, T., Sengupta, S., Ghosh, S., Sardana, K., 2016. Heterogeneity and antibiotic resistance in *Propionibacterium acnes* isolates and its therapeutic implications: blurring the lines between commensal and pathogenic phylotypes. Dermatol. Ther. 29 (6), 451–454.

Sampedro, M.F., Piper, K.E., McDowell, A., Patrick, S., Mandrekar, J.N., Rouse, M.S., Steckelberg, J.M., Patel, R., 2009. Species of Propionibacterium and *Propionibacterium acnes* phylotypes associated with orthopedic implants. Diagn. Microbiol. Infect. Dis. 64 (2), 138–145.

Scholz, C.F.P., Jensen, A., Lomholt, H.B., Brüggemann, H., Kilian, M., 2014. A novel high-resolution single locus sequence typing scheme for mixed populations of *Propionibacterium acnes* in vivo. PLoS One 9 (8), e104199.

Seper, A., Pressler, K., Kariisa, A., Haid, A.G., Roier, S., Leitner, D.R., Reidl, J., Tamayo, R., Schild, S., 2014. Identification of genes induced in *Vibrio cholerae* in a dynamic

biofilm system. Int. J. Med. Microbiol.: IJMM 304 (5-6), 749–763.
Sussman, M., Tang, Y.-W., 2014. Molecular Medical Microbiology: Three-volume-set, 2. Aufl. ed. Academic Press, [s.l.], 1 online resource.
Furustrand Tafin, U., Corvec, S., Betrisey, B., Zimmerli, W., Trampuz, A., 2012. Role of rifampin against *Propionibacterium acnes* biofilm in vitro and in an experimental foreign-body infection model. Antimicrob. Agents Chemother. 56 (4), 1885–1891.
Tunney, M.M., Dunne, N., Einarsson, G., McDowell, A., Kerr, A., Patrick, S., 2007. Biofilm formation by bacteria isolated from retrieved failed prosthetic hip implants in an in vitro model of hip arthroplasty antibiotic prophylaxis. J. Orthop. Res. 25 (1), 2–10.
Vorregaard, M., 2008. Comstat 2–a modern 3D image analysis environment for biofilms. Informatics and Mathematical Modelling. Technical University of Denmark, Kongens Lyngby, Denmark.